

Are your **MRI contrast agents** cost-effective?

Learn more about generic **Gadolinium-Based Contrast Agents**.



**FRESENIUS
KABI**

caring for life

AJNR

Contribution of Diffusion-Weighted Imaging in the Evaluation of Diffuse White Matter Ischemic Lesions in Fetuses: Correlations with Fetopathologic Findings

F. Guimiot, C. Garel, C. Fallet-Bianco, F. Menez, S.
Khung-Savatovsky, J.-F. Oury, G. Sebag and A.-L.
Delezoide

This information is current as
of April 18, 2024.

AJNR Am J Neuroradiol published online 18 October 2007
<http://www.ajnr.org/content/early/2007/10/18/ajnr.A0754.citation>

Contribution of Diffusion-Weighted Imaging in the Evaluation of Diffuse White Matter Ischemic Lesions in Fetuses: Correlations with Fetopathologic Findings

ORIGINAL RESEARCH

F. Guimiot
C. Garel
C. Fallet-Bianco
F. Menez
S. Khung-Savatovsky
J.-F. Oury
G. Sebag
A.-L. Delezoide



BACKGROUND AND PURPOSE: The sensitivity of fetal MR imaging is poor with regard to the evaluation of diffuse ischemic white matter (WM) abnormalities. Our purpose was to evaluate the contribution of diffusion-weighted imaging (DWI) in the analysis of microstructural changes in WM and to correlate neuroimaging with neurofetopathologic findings.

MATERIALS AND METHODS: We included fetuses with MR imaging, DWI, and a fetopathologic examination. In a region of interest defined by MR imaging, where T1 and T2 intensities were abnormal, the apparent diffusion coefficient (ADC) was measured and immunohistochemical analysis was performed. In fetuses with no WM abnormality in signal intensity, region of interest was defined at random. Histologic reading was performed with a complete blinding of the MR imaging results and ADC values. Three degrees of histologic appearance were defined with regard to vasogenic edema, astrogliosis, microgliosis, neuronal and oligodendrocytic abnormalities, and proliferation or congestion of vessels and were compared with a χ^2 test in groups A (normal ADC) and B (increased ADC) fetuses.

RESULTS: We included 12 fetuses in group A and 9 in group B, ranging from 29 to 38 weeks of gestation. All group B fetuses and 1 group A fetus demonstrated WM abnormalities in signal intensity. WM edema and astrogliosis were more common in group B than in group A (7/9 vs 2/12 and 8/9 vs 4/12, respectively). No significant difference was observed between both groups with regard to the other parameters.

CONCLUSION: This study showed a strong correlation between increased ADCs and 1) WM abnormalities in signal intensity on MR imaging, and 2) vasogenic edema with astrogliosis of the cerebral parenchyma.

The contribution of fetal MR imaging in the evaluation of cerebral ischemic lesions has already been evaluated.¹ MR imaging with the use of T2, T1, and T2*-weighted sequences has proved a valuable tool during the third trimester in the detection of small focal parenchymal lesions (such as cavitations and calcified leukomalacia) and ischemic lesions involving the cortex (4-layered polymicrogyria and laminar necrosis).^{1,2} Conversely, the sensitivity of MR imaging was poor in the evaluation of diffuse ischemic white matter (WM) abnormalities.¹ However, the detection of such lesions, before the establishment of irreversible damage, is challenging in at-risk situations.

Injury to the WM gives rise to neuronal hypoxia and, subsequently, to neuronal death, which results in disruption of the cell membrane and the release of some neurotransmitters such as glutamate. The latter has been demonstrated to have a cytotoxic effect on neurons.³ From this step begins microglial and astrogliosis responses. Microglial cells produce proinflammatory cytokines and reactive oxygen and nitrogen species that contribute to the strength of this deleterious effect.⁴

Astrocytes are recruited to repair the injured tissue and to reduce the effect of glutamate, resulting in a cellular swelling that corresponds to cytotoxic edema. A secondary vasogenic edema appears, caused principally by lysis of the astrocytic cell membrane and an opening in the blood-brain barrier, which induces an increase of the amount of water in the extracellular space.⁵ This vasogenic edema is present 1 week after the insult.⁶

The purpose of this study was to evaluate the contribution of diffusion-weighted imaging (DWI) in the evaluation of diffuse ischemic WM changes in fetuses, by correlating DWI and MR imaging with neurofetopathologic findings obtained by standard histologic and immunohistochemical analyses of the main cellular populations of the brain.

Materials and Methods


Experimental Procedures

All patients included in this retrospective study underwent fetal cerebral MR imaging with DWI. Termination of pregnancy (TOP) was performed in accordance with the French legislation and was followed by a fetopathologic examination. For each fetus, we recorded the main ultrasonographic and MR imaging findings, including the region of interest, where we measured the apparent diffusion coefficient (ADC). The gestational age at which TOP was performed, and the delay between MR imaging and fetopathologic examinations was also recorded. We performed a complete neuropathologic examination and undertook immunohistochemical studies at the level of the region of interest, to achieve histologic and MR image matching. We obtained histologic results with a complete blinding of the MR imag-

Received May 12, 2007; accepted May 15.

From the Service de Biologie du Développement (F.G., F.M. S.K.-S., A.-L.D.), Service de Radiologie (G.S., C.G.), and Service de Gynécologie-Obstétrique (J.-F.O.), Hôpital Robert Debré, AP-HP, Paris, France; and the Service d'Anatomie Pathologique (C.F.-B.), Hôpital Saint-Anne, Paris, France.

Please address correspondence to Anne-Lise Delezoide, Service de Biologie du Développement, Hôpital Robert Debré, 48 Boulevard Sérurier, 75019 Paris, France; e-mail: anne-lise.delezoide@rdp.aphp.fr

 Indicates article with supplemental on-line tables.

DOI 10.3174/ajnr.A0754

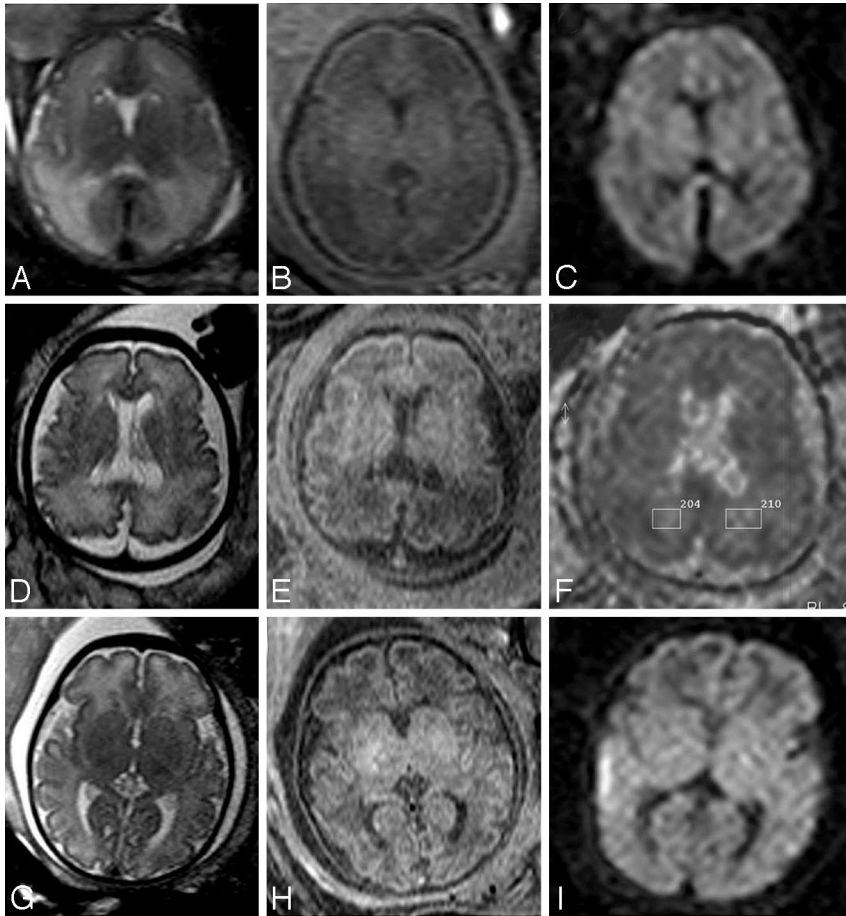


Fig 1. Correlation between WM MR signals and DWI abnormalities is shown on T1 (A,D,G), T2 (B,E,H), ADC map (F), and DWI (C,I) axial sections of the brains of group A and group B fetuses. A–C, Case 11 demonstrates marked diffuse T1 hypointensity and T2 hyperintensity of the WM with normal diffusion. D–F, Case 5 shows mild T1 hypointensity and T2 hyperintensity of the posterior WM with increased ADCs (2.10). G–I, Case 6 exhibits more marked T1 hypointensity and T2 hyperintensity of the anterior WM with increased diffusion.

ing results and ADC values. We subsequently performed confrontation of MR imaging and histologic results.

MR Imaging and DWI

We performed MR imaging on a 1.5T unit (Intera; Philips Medical Systems, Best, the Netherlands) 30 to 40 minutes after fetal sedation was achieved with maternal oral administration of flunitrazepam (1 mg). We performed a brain examination with a phased-array abdominal coil, T1-weighted spin-echo, spectral presaturation inversion recovery, fat-saturated sequences (697/14/2; flip angle, 90°; matrix: 256 × 256; FOV, 320 mm; rectangular FOV, 75%; section thickness, 4 mm; acquisition time, 2 min 56 s) and T2-weighted single-shot turbo spin-echo imaging (24,617/100/1; flip angle, 90°; turbo spin-echo factor, 84; matrix: 256 × 256; FOV, 280 mm; section thickness, 3 mm; acquisition time, 24 s). DWI was acquired without maternal breath-hold on transverse sections with a multishot echo-planar imaging sequence with diffusion gradient (TR, 3341 ms; TE, 88 ms; flip angle, 90°; matrix, 95 × 256 mm; FOV, 280 mm; section thickness, 5 mm; b-values of 0 and 700 s/mm² applied in 6 noncollinear directions; amplitude, 30mT/m; acquisition time, 53 s) (Fig 1). The same radiologist (C.G.) manually traced a rectangular region of interest (region of interest size varied from 100 to 150 mm²) in the region where the WM signal intensity was abnormal, on the image obtained with b = 0 s/mm². If the signal intensity was normal, the site where ADC was traced was sampled at random. The ADC was calculated according to the equation: $S(b) = S(0) \cdot \exp(-b \times \text{ADC})$ where S(b) is signal intensity at a b value and S(0) is signal intensity without diffusion gradients. In reference with normal published data in fetuses,^{7,8} ADC was considered normal when it was strictly inferior to 2.10 μm²/ms and in-

creased when it was superior or equal to this value. Two groups were defined: fetuses with normal ADC (group A) and fetuses with increased ADC (group B).

Termination of Pregnancy

We obtained TOP by performing feticide (injection of 5 U/mL of pentothal or 5 U/mL of KCl into the vein of the fetal umbilical cord) followed by induction of labor. Delivery usually occurred within 24 hours after feticide, and a fetopathologic examination was performed within 24 hours after delivery, which allowed good brain preservation.

Fetopathologic Examination

After the parents' informed consent and in accordance with the French legislation, we obtained fetal brains from medically terminated pregnancies. The gestational ages of the fetuses was established by first-trimester sonography crown-rump length measurement and confirmed at autopsy by the evaluation of the fetal biometry, and organ and skeletal maturation. Brains were removed and fixed in 10% buffered formalin added with 3 g/L of ZnSO₄ for approximately 3 to 4 weeks. Brains were then cut in coronal sections of 0.5 cm of thickness for routine examination. The region of interest identified by MR imaging was sampled, cut in several parts (from 2 to 3 blocks), and embedded in paraffin. Serial sections (thickness 4 μm) were performed on Superfrost Plus slides (Thermo Scientific, Waltham, Mass). One section was stained with hematoxylin-eosin (H&E) for histologic analysis.

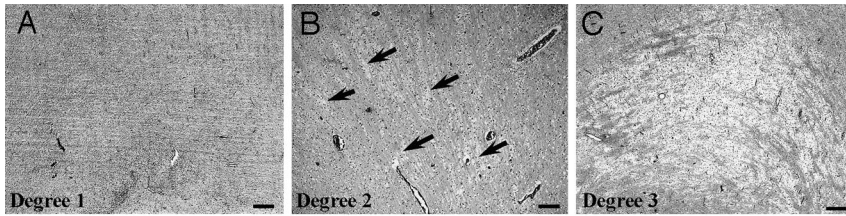
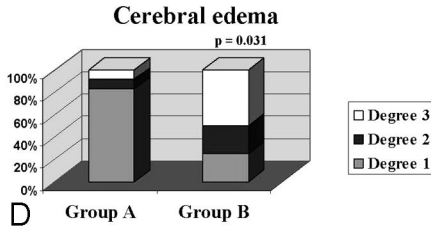


Fig 2. Histologic analysis for cerebral edema. Histologic sections stained with H&E show the 3 degrees of cerebral edema (A–C). A, Degree 1 edema. B, Degree 2 edema (arrows indicate mild parenchymal dissociation). C, Degree 3 edema. D, A 3D graphic representation of the distribution of the 3 degrees of cerebral edema between the 2 groups. Scale bars indicate 400 μm .



Immunohistochemical Examination

We performed all incubations in a humidified chamber. First, sections were dewaxed with xylene and bathed consecutively in absolute ethanol, 75% ethanol, 35% ethanol, and H₂O. Then, they were incubated for 30 minutes at 95 to 98°C in 10 mmol/L sodium citrate, pH 6.0, for antigen retrieval, and cooled for 20 minutes at room temperature. Next, endogenous peroxidase activity was inactivated for 5 minutes in 3% hydrogen peroxide. Sections were then washed 3 times in phosphate-buffered saline (PBS) and blocked 30 minutes in PBS, 3% BSA, 0.1% Tween 20 (Sigma, St Louis, Mo), before incubation with primary antibodies overnight at 4°C. The next morning, the LSAB2 streptavidin-biotin detection system kit (Dako, Trappes, France) was used to reveal immunolabeling. Sections were washed 3 times in PBS, 0.1% Tween 20, before adding secondary and tertiary antibodies (biotin-conjugated anti-mouse or anti-rabbit and peroxidase-conjugated streptavidin, respectively) for 1 hour at room temperature. DAB (3,3'-diaminobenzidine tetrahydrochloride, Dako) was used as a substrate for peroxidase, and incubation was performed for 5 to 10 minutes. Negative controls were tissue sections incubated without primary antibody and concentration-matched secondary and tertiary antibodies. Sections were counterstained with Mayer hemalun and mounted in PERTEX medium (Histolab Products, Gothenburg, Sweden). Sections were analyzed on a DMR microscope (Leica, Heidelberg, Germany), and images were acquired with a DFW-SX900 camera (Sony, Tokyo, Japan) and Inspector software (Matrox Imaging, Quebec, Canada). Primary antibodies were mouse anti-human CD34 (Immunotech, Marseille, France), microtubule-associated protein 2 (MAP2) (Sigma, Lyon, France), CD45, glial fibrillary acidic protein (GFAP) and nuclear factor (NF) (all from Dako), rabbit anti-human myelin basic protein (MBP) (Dako), and OLIG2 (Chemicon, UK).

Histologic Evaluation

For histologic and immunohistochemical evaluations, 2 pathologists (F.G., C.F.-B.) separately analyzed all sections, with common reevaluation when necessary.

Standard staining and immunohistochemical examination allowed us to define 3 degrees of intensity of vasogenic edema (corresponding to a WM dissociation resulting from an increase in extracellular water), microgliosis, astrogliosis, and proliferation or congestion of vessels. For edema, “degree 1” corresponds to an absence of edema, “degree 2” to a mild dissociation of WM nervous fibers, and “degree 3” to a severe dissociation of WM nervous fibers with the appearance of empty zones. For astrogliosis, “degree 1” cor-

responds to a few round and swollen astrocytes observed among normal starry astrocytes, “degree 2” to increased number of round and swollen astrocytes, and “degree 3” to only round and swollen astrocytes. For microgliosis and proliferation or congestion of vessels, “degree 1” corresponds to only nonreactive resident microglial cells without proliferation or congestion of vessels, “degree 2” to more numerous nonreactive microglial cells compared with degree 1 and mild proliferation or congestion of vessels, and “degree 3” to an increased number of round reactive microglial cells associated with microglial nodules and high proliferation or congestion of vessels. We then statistically compared the distribution of the 3 degrees of each parameter in group A and B fetuses. We evaluated the integrity of WM neurons and oligodendrocytes by counting and analyzing their morphologic appearance. Five microscopic nonoverlapping fields were analyzed for each slide. Neurons were classified as necrotic when they exhibited pyknosis, karyorrhexis, karyolysis, cytoplasmic eosinophilia (“dark neuron”), or loss of affinity for hematoxylin (“ghost neuron”).

Statistics

We performed statistical analysis using Excel (Microsoft, Redmond, Wash) and Prism 4 (GraphPad, San Diego, Calif) software. A χ^2 test was performed on the percentage of distribution of histologic degree among the fetuses in groups A and B. We compared the averages of gestational ages and of the delay between MR imaging and fetopathologic examinations in both groups with a Student *t* test to eliminate differences that could have biased the study. A probability value of *P* < .05 was considered statistically significant.

Results

Between 2002 and 2005, we included 21 fetuses (12 female and 9 male) in this study. Group A included 12 fetuses and group B, 9 fetuses. MR imaging was performed at a mean gestational age of 32 weeks. The gestational ages of the fetuses at TOP ranged from 29 to 38 weeks; the average was 33.38 ± 0.66 weeks for group A and 34.71 ± 0.83 weeks for group B (*P* = .24). To ensure that no difference in the delay of MR imaging and fetopathologic examinations could be observed between both groups and therefore could distort the results, we compared the mean delay in the 2 groups: 16.38 ± 3.55 days for group A and 10.25 ± 2.35 days for group B (*P* = .22). The results are summarized in on-line Tables 1 and 2.

It is noteworthy that WM MR imaging abnormalities in signal intensity (T1 hypointensity and T2 hyperintensity) were

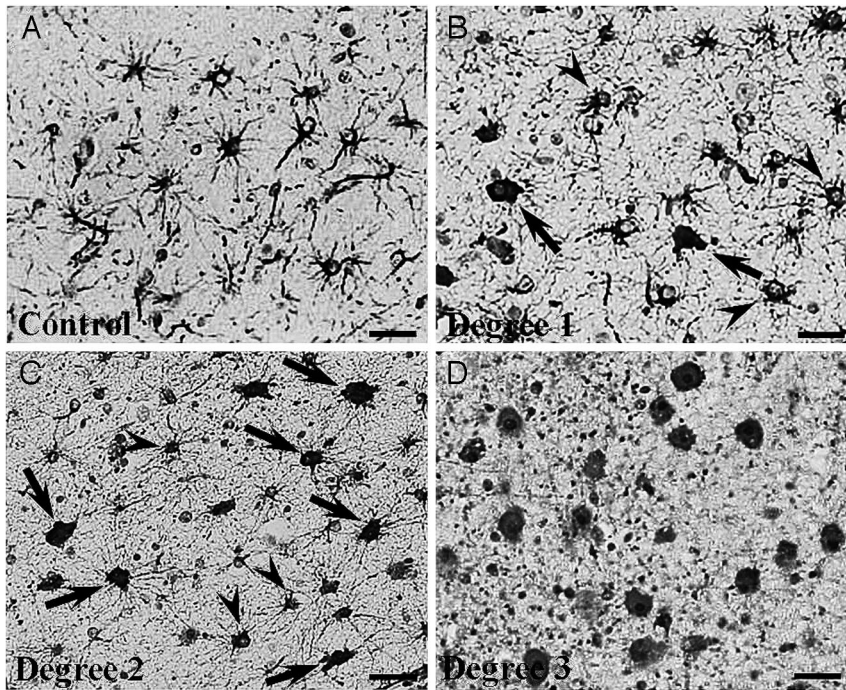
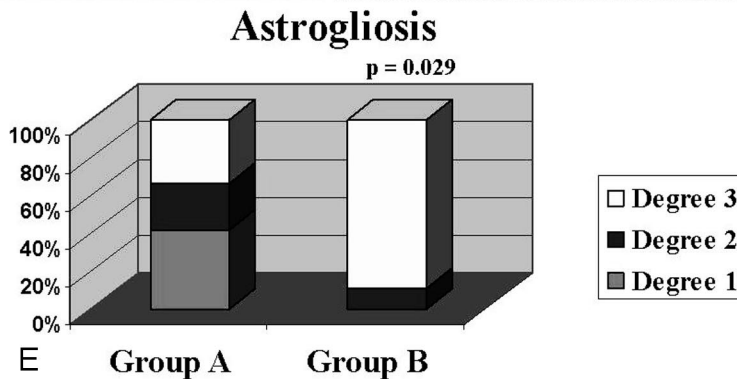


Fig 3. Histologic analysis for astrogliosis. Immunohistochemical examination of astrogliosis with a GFAP-specific antibody (A–D). A, Normal astrocytic population. B, Degree 1 astrogliosis. C, Degree 2 astrogliosis (arrowheads and arrows indicate normal astrocytes and reactive astrocytes, respectively, in B and C). D, Degree 3 astrogliosis. E, A 3D graphic representation of the distribution of the 3 degrees of astrogliosis between the 2 groups. Scale bars indicate 50 μ m.



observed in all group B fetuses and in only 1 group A fetus (case 11, on-line Table 1).

Vasogenic Edema

We studied and evaluated vasogenic edema on sections stained with H&E in the 2 groups of fetuses. We delineated 3 degrees of edema (see Materials and Methods): “degree 1” (Fig 2A), “degree 2” (Fig 2B), and “degree 3” (Fig 2C). Statistical analysis of the distribution of the 3 degrees of edema in the fetuses of both groups allowed us to find that degrees 2 and 3 edema were significantly more common in group B (7/9, 77.8%) than in group A (2/12, 16.7%) ($P = .031$) (Fig 2D).

Astrogliosis

Using GFAP immunohistochemistry, we delineated 3 degrees of astroglial response: “degree 1” (Fig 3B), “degree 2” (Fig 3C), and “degree 3” (Fig 3D). Normal starry astrocytes were also included (Fig 3A). Increased astrogliosis was observed mainly in group B fetuses. More cases with degree 3 astrogliosis were found in group B (8/9, 88.9%) than in group A (4/12, 33.3%) ($P = .029$) (Fig 3E). Moreover, no degree 1 astrogliosis was observed in group B, but it was found in 5 of 12 fetuses in group A (41.7%).

Microgliosis, Neuronal and Oligodendrocytic Abnormalities, and Proliferation or Congestion of Vessels

Using CD45 immunohistochemical and standard histologic examinations, we defined 3 degrees of histologic appearance according to microgliosis and proliferation or congestion of vessels. The distribution of these degrees was analyzed, but no significant statistical difference was observed between both groups.

Using standard histologic evaluation and NF, MAP2, OLIG2, and MBP immunohistochemical methods, we evaluated the number and integrity of interstitial neurons and oligodendrocytes to take into account cellular loss or morphologic changes. No significant difference was observed between both groups (data not shown).

Discussion

The detection of WM lesions in the early stages of hypoxic-ischemic damage, before the establishment of irreversible lesions, is of paramount importance in the determination of appropriate pregnancy management, or accurate fetal prognosis. MR imaging should have a key role in this field because the clinical and biologic contribution is limited and sonography has a poor sensitivity. In fetuses, some at-risk situations

may lead to an impairment of brain perfusion and subsequent cerebral ischemia. In the prenatal period, although acute events such as in utero death of 1 monozygotic twin or maternal hypovolemic shock or trauma rarely happen, unlike what is observed in the postnatal period, chronic damage is much more common and may be related mainly to placental insufficiency or maternofetal infection.⁹ MR imaging with T2, T1, and T2*-weighted sequences has proved to be valuable in the detection of focal ischemic WM lesions but much less accurate in the detection of diffuse WM abnormalities.¹ Indeed, because of high water content and incomplete myelination of the fetal brain in utero, WM shows a physiologic T1 hypointensity and T2 hyperintensity. So, on the basis of signal intensity analysis only, it is very difficult to assert with any certainty the presence of diffuse ischemic lesion lengthening on both T1 and T2 sequences. In our study, there was a good agreement between WM MR imaging signal intensity and abnormalities in the ADCs. In only 1 case (case 11, group A), discussed below, ADC was normal despite marked T1 hypointensity and T2 hyperintensity (Figs 1A–C). Evaluation of signal intensity remains subjective and difficult, as described above, and ADC measurement provides a more objective way of analyzing the cerebral parenchyma.

The contribution of DWI in evaluation of perinatal brain injury has been studied widely in neonates, and the DWI patterns of lesions reflecting microstructural changes in the WM and basal ganglia have been described.^{10–12} So far, little is known about DWI in the fetal brain. Mean normal values of ADC have been reported in 2 small series,^{7,8} but no study has evaluated the contribution of DWI in the detection of WM ischemic damage.

Correlations between DWI and histologic lesions in the ischemic brain have been reported in experimental studies, mainly with animal models of focal ischemic stroke.¹³ In light of these experiments, it has been stated that acute brain injury is responsible for disruption of water and electrolyte homeostasis, ensuing cellular swelling and cytotoxic edema. Therefore, the initial decrease in ADC results from a shift of water from the extracellular to the intracellular space; water in the extracellular space is supposed to have a higher diffusion coefficient than water in the intracellular space. Secondary loss of integrity of the cell membrane and cell lysis are responsible for increases in the volume of the extracellular space, vasogenic edema, and subsequent increased ADC. During this transition from acute to subacute and chronic injury, a period of DWI pseudonormalization is observed during which the histologic damage persists.^{14,15} Swollen astrocytes rather than shrunken neurons could be the major contributor to the initial reduction in ADC.¹³ Most experimental studies with animal models are based on an acute external injury and therefore do not reproduce the sequence of events arising in fetuses. In a recently published study,¹⁶ WM lesions were induced in neonatal rats by prolonged exposition under protracted prenatal hypoxia, until the day before delivery. Neonatal rat brains were investigated by *in vivo* DWI and standard histologic and immunohistochemical evaluations from the day of birth to the twenty-first day. Prenatal hypoxia was associated with cystic-like lesions of WM, more numerous macrophages, severe astrogliosis, increased cell death, and enhanced angiogenesis. These changes were observed mostly before the seventh day

after birth. On this day, ADC values were significantly increased compared with the control group, whereas T2 and T1 densities were not significantly different in the control and hypoxic groups. The conditions of this study were very similar to what is observed in fetuses with chronic brain damage and suggest that increased ADC may precede modifications of WM MR imaging signal intensity.

Our study shows a correlation between increased ADC and the presence of vasogenic edema and astrogliosis. These results are in agreement with what has been reminded above (correlations between DWI and histologic findings) and with Baud's experiments.¹⁶ It is noteworthy that in all cases with increased ADC, abnormalities in signal intensity of the WM were also present, which is not surprising because vasogenic edema also generates changes in signal intensity of the WM.¹³ In some cases, abnormalities in WM were marked, whereas in other cases, they were more subtle. Normal variants in the signal intensity of the WM are not well known in fetuses,¹⁷ so that in these questioning cases, the use of DWI might be helpful because determination of ADC provides a more objective way of evaluating the integrity of the WM.

In 4 cases (cases 5 and 11, group A; cases 4 and 7, group B), there was a disagreement between MR imaging and histologic results. In case 5, the delay between the 2 examinations was 16 days, and the edema might have developed during the days after MR imaging. In case 11, signal intensity and histologic abnormalities were marked, whereas ADC was within the normal range (Figs 1A–C). As usual, there was no known acute causal event, so that we do not know when the injury started, but an explanation for the disagreement between the 2 methods might be the fact that DWI was performed during the phase of pseudonormalization. We could not find any explanation for cases 4 and 7.

Increased microgliosis was observed in 7 fetuses (cases 9, 10 and 11, group A; and cases 2, 3, 4, and 9, group B). In all cases, except for 2 (cases 9 and 10, group A), fetuses presented with intrauterine growth restriction or cytomegalovirus infection. Four fetuses showed increased ADC. These findings correlate well with the results of Baud's study.¹⁶

Conversely, we could not find any correlation between increased ADC and neuronal or oligodendrocytic modifications and proliferation or congestion of vessels. However, absence of increased neuronal death is not surprising in a case of chronic injury; indeed, a recent study has shown that under chronic ischemic conditions, neuronal death was prevented by increased connexin-43 expression.¹⁸ This protein might have neuroprotective effects and would be produced by astrocytes in response to hypoxic stimulation. Furthermore, oligodendrocytes are most vulnerable to hypoxic-ischemic brain injury, but, in our study, we did not observe any decrease in the oligodendrocytic population. This finding could be explained by oligodendrocytic proliferation as demonstrated by Zaidi et al,¹⁹ who observed, in rodents, a generation of new oligodendrocytes after a hypoxic-ischemic brain injury. The absence of vascular changes may also be observed in association with cerebral edema, and it has been shown that the blood-brain barrier opening was clearly not required for edematous formation.²⁰ Moreover, low vessel density in the deep WM emphasizes the hypothesis that cerebral edema is not induced by the blood-brain barrier opening.²¹

It is difficult to evaluate the contribution of the process of TOP in neuropathologic lesions. This process could affect the brain, and, for example, if the delay between feticide and delivery is longer than 48 hours, cellular lysis starts in utero and tissues are injured. However, in our cases this delay did not exceed 24 to 48 hours. Furthermore, the drug (oxytocin) used for inducing delivery generates uterine contractions that may affect the fetal brain (when they are numerous or extensive) by increasing blood pressure and may be responsible for vascular defects in the brain.²² Nevertheless, in our study, both groups had the same constraints and therefore may be compared.

Our results may be biased by the small number of fetuses and the delay, sometimes rather long (notably in cases 1, 3, 4, 5, 6, and 10 of group A and cases 3 and 7 of group B) between MR imaging and TOP. This long delay (superior to 2 weeks) may account for some disagreement between the findings on MR imaging and the fetopathologic findings.

Conclusion

Our preliminary study provides very interesting information about the role of DWI in the evaluation of fetuses with diffuse hypoxic-ischemic damage to the WM, which is one of the most challenging situations encountered in prenatal diagnosis. Evaluation of diffuse WM injuries with MR imaging on the basis of signal intensity abnormalities only is always subjective and difficult. Measurement of ADC provides a more objective way of analyzing the fetal WM. The presence of a strong correlation between increased ADC and cerebral edema with astrogliosis emphasizes the necessity of DWI in the evaluation of diffuse hypoxic-ischemic WM injury in fetuses. The prognosis of WM abnormalities in signal intensity with increased ADC is unknown, and the postnatal follow-up of children presenting with these findings during the prenatal period will undoubtedly be of paramount importance.

Acknowledgments

We thank Drs M. Bucourt, M. Catala, Y. Hutten, Ph. Rouvier, and the late F. Daikha-Dahmane for their contribution to this study. We also thank M.N. Lotiquet and B. Bartolt for their technical assistance, and Vincent Delezoide for correcting the manuscript.

References

1. Garel C, Delezoide AL, Elmaleh-Berges M, et al. Contribution of fetal MR imaging in the evaluation of cerebral ischemic lesions. *AJNR Am J Neuroradiol* 2004;25:1563–68
2. Righini A, Zirpoli S, Mrakic F, et al. Early prenatal MR imaging diagnosis of polymicrogyria. *AJNR Am J Neuroradiol* 2004;25:343–46
3. Choi DW, Rothman SM. The role of glutamate neurotoxicity in hypoxic-ischemic neuronal death. *Annu Rev Neurosci* 1990;13:171–82
4. Hao AJ, Dheen ST, Ling EA. Expression of macrophage colony-stimulating factor and its receptor in microglia activation is linked to teratogen-induced neuronal damage. *Neuroscience* 2002;112:889–900
5. Landis DM. The early reactions of non-neuronal cells to brain injury. *Annu Rev Neurosci* 1994;17:133–51
6. Matsumoto K, Lo EH, Pierce AR, et al. Role of vasogenic edema and tissue cavitation in ischemic evolution on diffusion-weighted imaging: comparison with multiparameter MR and immunohistochemistry. *AJNR Am J Neuroradiol* 1995;16:1107–15
7. Bui T, Daire JL, Chalard F, et al. Microstructural development of human brain assessed in utero by diffusion tensor imaging. *Pediatr Radiol* 2006;36:1133–40
8. Righini A, Bianchini E, Parazzini C, et al. Apparent diffusion coefficient determination in normal fetal brain: a prenatal MR imaging study. *AJNR Am J Neuroradiol* 2003;24:799–804
9. Girard N, Gire C, Sigaudy S, et al. MR imaging of acquired fetal brain disorders. *Childs Nerv Syst* 2003;19:490–500
10. Hüppi PS, Dubois J. Diffusion tensor imaging of brain development. *Semin Fetal Neonatal Med* 2006;11:489–97
11. Robertson RL, Ben-Sira L, Barnes PD, et al. MR line-scan diffusion-weighted imaging of term neonates with perinatal brain ischemia. *AJNR Am J Neuroradiol* 1999;20:1658–70
12. Rutherford M, Srinivasan L, Dyet L, et al. Magnetic resonance imaging in perinatal brain injury: clinical presentation, lesions and outcome. *Pediatr Radiol* 2006;36:582–92
13. Rivers CS, Wardlaw JM. What has diffusion imaging in animals told us about diffusion imaging in patients with ischaemic stroke? *Cerebrovasc Dis* 2005;19:328–36
14. Neil J, Miller J, Mukherjee P, et al. Diffusion tensor imaging of normal and injured developing human brain—a technical review. *NMR Biomed* 2002;15:543–52
15. Sotak CH. Nuclear magnetic resonance (NMR) measurement of the apparent diffusion coefficient (ADC) of tissue water and its relationship to cell volume changes in pathological states. *Neurochem Int* 2004;45:569–82
16. Baud O, Daire JL, Dalmaz Y, et al. Gestational hypoxia induces white matter damage in neonatal rats: a new model of periventricular leukomalacia. *Brain Pathol* 2004;14:1–10
17. Garel C. New advances in fetal MR neuroimaging. *Pediatr Radiol* 2006;36:621–25
18. Nakase T, Yoshida Y, Nagata K. Enhanced connexin 43 immunoreactivity in penumbral areas in the human brain following ischemia. *Glia* 2006;54:369–75
19. Zaidi AU, Bessert DA, Ong JE, et al. New oligodendrocytes are generated after neonatal hypoxic-ischemic brain injury in rodents. *Glia* 2004;46:380–90
20. Beaumont A, Marmarou A, Hayasaki K, et al. The permissive nature of blood brain barrier (BBB) opening in edema formation following traumatic brain injury. *Acta Neurochir Suppl* 2000;76:125–29
21. Miyawaki T, Matsui K, Takashima S. Developmental characteristics of vessel density in the human fetal and infant brains. *Early Hum Dev* 1998;53:65–72
22. Li H, Gudmundsson S, Olofsson P. Acute centralization of blood flow in compromised human fetuses evoked by uterine contractions. *Early Hum Dev* 2006; 82:747–52

Table 1: Imaging, fetopathologic, and immunohistologic findings in group A fetuses

Case	US Findings	MR Findings	(ADC, $\mu\text{m}^2/\text{ms}$)	WM ROI	MR/Fetopathologic Examinations Delay (days)	GA at TOP (weeks)	Neuropathologic Findings	Immunohistologic Results	Placental Findings
1	Mild bilateral ventriculomegaly	Bilateral ventriculomegaly (15 mm on the right and 13 mm on the left), subependymal heterotopia, cavitation, WM: normal	1.54	Right frontal	35	36	Mild bilateral ventriculomegaly, subependymal heterotopia	A: +++ E: + M: 0 N: 0 O: 0 V: +++	No abnormality
2	Intraventricular hemorrhage, frontal calcification	Polymicrogyria, calcified leukomalacia, WM: normal	1.40	Right frontal	3	30	Polymicrogyria, calcified intraventricular hemorrhage	A: ++ E: + M: ++ N: 0 O: 0	No abnormality
3	Suspicion of lissencephaly	Lissencephaly, WM: normal	1.65	Left frontal	17	32	Microcephaly with simplified gyral pattern	A: ++ E: 0 M: + N: 0 O: 0 V: +	Placental hypotrophy, vascular lesions
4	Mild bilateral ventriculomegaly	Bilateral ventriculomegaly (14.6 mm on the right and 15 mm on the left), WM: normal	1.75	Right frontal	18	34	Mild bilateral ventriculomegaly, mild aqueductal stenosis	A: ++ E: + M: 0 N: 0 O: 0 V: +++	Partial circumvallate, small infarcts (10 % of volume)
5	Suspicion of partial vermian agenesis	Partial vermian agenesis, WM: normal	1.68	Left frontal	16	35	Mild unilateral ventriculomegaly, partial vermian agenesis	A: +++ E: ++ M: 0 N: 0 O: 0 V: ++	No abnormality
6	Cervical cystic lymphangioma	Lingual extension of the cystic lymphangioma, WM: normal	1.80	Right frontal	17	34	No cerebral abnormalities	A: ++ E: + M: + N: 0 O: 0 V: ++	No abnormality
7	Severe unilateral ventriculomegaly	Left unilateral ventriculomegaly (35.7 mm), WM: normal	1.62	Right frontal	6	37	Severe unilateral ventriculomegaly	A: + E: 0 M: + N: 0 O: 0 V: ++	No abnormality
8	Fetal hypokinesia	No structural abnormalities, WM: normal	1.75	Right frontal	23	33	Micrencephaly, arhinencephaly	A: +++ E: 0 M: + N: 0 O: 0 V: +	No abnormality
9	Corpus callosum agenesis, suspicion of posterior fossa abnormality	Corpus callosum agenesis, vermian hypoplasia, WM: normal	1.70	Right temporal	4	34	Corpus callosum agenesis, vermian hypoplasia, mild unilateral ventriculomegaly	A: + E: + M: + N: 0 O: 0 V: +	No abnormality
10	Cardiac rhabdomyoma, suspicion of Bourneville tuberous sclerosis	Subependymal tubers, WM: normal	2.00	Right occipital	47	36	WM, subependymal and cortical tubers	A: + E: 0 M: +++ N: 0 O: 0 V: +	Placental hypotrophy
11	IUGR, Doppler abnormalities	Subependymal pseudocysts, WM: *T1, **T2 (Figs 1A-C)	1.70	Left parieto-occipital	4	31	Delayed gyration, subependymal pseudocysts	A: + E: +++ M: +++ N: 0 O: 0 V: +++	Placental hypotrophy, voluminous subchorionic thrombosis
12	Toxoplasmosis seroconversion	Focal parenchymal lesions, WM: normal	1.64	Left frontal	6	29	Necrotic focal parenchymal lesions	A: + E: 0 M: + N: 0 O: 0 V: ++	Granulomatous villitis

Note:—Immunohistochemical signal intensity was evaluated as mild (+), moderate (++) and high (+++). 0 indicates absence of abnormality; A, astrogliosis; E, edema; IUGR, intrauterine growth restriction; M, microgliosis; N, neuronal abnormalities; O, oligodendrocytic abnormalities; US, ultrasonography; WM, white matter; ROI, region of interest; ADC, apparent diffusion coefficient; GA, gestational age; TOP, termination of pregnancy; V, vessel proliferation or congestion; *T1, T1 hypointensity; **T2, T2 hyperintensity.

Table 2: Imaging, fetopathologic, and immunohistologic findings in group B fetuses

Case	US Findings	MR Findings	(ADC, $\mu\text{m}^2/\text{ms}$)	WM ROI	MR/Feto-pathologic Examinations Delay (days)	GA at TOP (weeks)	Neuropathologic Findings	Immunohistologic Results	Placental Findings
1	Severe bilateral ventriculomegaly	Intraventricular and parenchymal hemorrhage, WM: *T1, **T2	2.20	Left frontal	2	35	Severe bilateral ventriculomegaly, intraventricular and parenchymal hemorrhage	A: +++ E: +++ M: + N: 0 O: 0 V: +++	Placental hypotrophy, mild ischemia
2	IUGR, Doppler abnormalities	No structural abnormalities, WM: *T1, **T2	2.25	Left parieto-occipital	5	33	WM edema	A: ++ E: ++ M: +++ N: 0 O: 0 V: +	Velamentous cord insertion
3	Mild left ventriculomegaly, CMV infection, PCR +	Left ventriculomegaly (12.8 mm), ventricular septation, WM: *T1, **T2	2.28	Left frontal	20	38	Mild bilateral ventriculomegaly, subependymal pseudocysts, viral inclusions	A: +++ E: + M: +++ N: 0 O: 0 V: ++	Chronic villitis, no viral inclusions
4	CMV infection, PCR +	No structural abnormalities, WM: *T1, **T2	2.25	Left frontal	6	32	Subependymal pseudocysts, viral inclusions	A: +++ E: + M: +++ N: 0 O: 0 V: +	Specific chronic villitis, viral inclusions
5	Familial history of Joubert syndrome, severe unilateral ventriculomegaly	Left ventriculomegaly (14 mm), WM: normal T1, **T2 (Figs 1D-F)	2.10	Left parieto-occipital	14	33	Mild unilateral ventriculomegaly	A: +++ E: ++ M: + N: 0 O: 0 V: +	Circummarginate placenta
6	Maternal CMV seroconversion, mild unilateral ventriculomegaly, bilateral subependymal pseudocysts, PCR -	Bilateral ventriculomegaly (both 13 mm), bilateral subependymal pseudocysts, WM: *T1, **T2 (Figs 1G-I)	2.20	Right frontal	8	35	Mild bilateral ventriculomegaly, bilateral subependymal pseudocysts, no viral inclusions, no fetal infection	A: +++ E: + M: + N: 0 O: 0 V: ++	No abnormality
7	Mild bilateral ventriculomegaly, subependymal pseudocysts	Subependymal pseudocysts, WM: *T1, **T2	2.25	Right occipital	20	37	Bilateral subependymal pseudocysts, macrencephaly, wide cavum	A: +++ E: + M: + N: 0 O: 0 V: +	No abnormality
8	IUGR, Doppler abnormalities	Delayed gyration, WM: *T1, **T2	2.40	Right frontal	11	33	Delayed gyration	A: +++ E: +++ M: + N: 0 O: 0 V: +	Placental hypotrophy, villous ischemic change
9	Mild bilateral ventriculomegaly, CMV infection PCR +	Bilateral ventriculomegaly (14.1 mm on the right and 13.4 mm on the left), WM: *T1, **T2	2.39	Right parieto-occipital	10	38	Mild bilateral ventriculomegaly, viral inclusions	A: +++ E: +++ M: +++ N: 0	Specific chronic villitis, viral inclusions

Note:—Immunohistochemical signal intensity was evaluated as mild (+), moderate (++) and high (+++). 0 indicates absence of abnormality; A, astrogliosis; E, edema; CMV, cytomegalovirus; IUGR, intrauterine growth restriction; M, microgliosis; N, neuronal abnormalities; O, oligodendrocytic abnormalities; PCR, polymerase chain reaction in amniotic fluid; US, ultrasonography; WM, white matter; ROI, region of interest; ADC, apparent diffusion coefficient; GA, gestational age; TOP, termination of pregnancy; V, vessel proliferation or congestion; *T1, T1 hypointensity, **T2, T2 hyperintensity.